Seasonal fluxes of carbonyl sulfide in a midlatitude forest

The Harvard community has made this article openly available. **Please share** how this access benefits you. Your story matters

Citation	Commane, Róisín, Laura K. Meredith, Ian T. Baker, Joseph A. Berry, J. William Munger, Stephen A. Montzka, Pamela H. Templer, Stephanie M. Juice, Mark S. Zahniser, and Steven C. Wofsy. 2015. "Seasonal Fluxes of Carbonyl Sulfide in a Midlatitude Forest." Proc Natl Acad Sci USA 112 (46) (November 2): 14162–14167. doi:10.1073/pnas.1504131112.
Published Version	doi:10.1073/pnas.1504131112
Citable link	http://nrs.harvard.edu/urn-3:HUL.InstRepos:27715927
Terms of Use	This article was downloaded from Harvard University's DASH repository, and is made available under the terms and conditions applicable to Other Posted Material, as set forth at http://nrs.harvard.edu/urn-3:HUL.InstRepos:dash.current.terms-of-use#LAA

1
2
3
4
5
6
7
8
9
10
11
12
13
14
15
16
17
18
19
20
21
22
23
24
25
26
27
28
29
30
31
32
33
34
35
36
37
38
39
40
41
42
43
44
45
46
47
48
49
50
51
52
53
54
55
56
57
58
59
60
61
62
63
64
65
66
67
68
69
70
71
72
73
74
75
76
77
78
79
80
81
82
83
84
85
86
87
88
89
90
91
92
93
94
95
96
97
98
99
100
101
102
103
104
105
106
107
108
109
110
111
112
113
114
115
116
117
118
119
120
121
122
123
124
125
126
127
128
129
130
131
132
133
134
135
136

Seasonal fluxes of carbonyl sulfide in a mid-latitude forest

Róisín Commane[1]*, Laura K. Meredith[2], Ian T. Baker[3], Joseph A. Berry[4], J. William Munger[1], Stephen A. Montzka[5], Pamela H. Templer[6], Stephanie M. Juice[6], Mark S. Zahniser[7], Steven C. Wofsy[1]

[1]Harvard School of Engineering and Applied Sciences and Dept. Earth and Planetary Sciences, Harvard University, Cambridge, MA. [2]Massachusetts Institute of Technology, Cambridge, MA; now at Stanford School of Earth, Energy & Environmental Sciences, Stanford, CA [3]Dept. of Atmospheric Science, Colorado State University, Fort Collins, CO [4]Dept. of Global Ecology, Carnegie Institution, Stanford, California, USA [5]Global Monitoring Division, NOAA Earth System Research Laboratory, Boulder, CO [6]Dept. of Biology, Boston University, Boston, MA [7]Aerodyne Research Inc., Billerica, MA

Carbonyl sulfide (OCS) is the most abundant sulfur gas in the atmosphere. Atmospheric mixing ratios of OCS have shown a summer minimum associated with vegetative uptake, closely correlated with CO_2. We report the first direct measurements of the ecosystem flux of OCS throughout an annual cycle above a mixed temperate forest. The forest took up OCS during most of the growing season with an annual uptake of -43.5 ± 0.5 gS ha^{-1} (95% confidence interval). Night-time fluxes accounted for 28% of the total uptake, with contributions from soils and incompletely closed stomata of plants. Unexpected net OCS emission occurred during the warmest weeks in summer. Many requirements necessary to use OCS as a simple estimate of photosynthesis were found to be invalid as OCS fluxes did not have a constant relationship with photosynthesis throughout the day or over the seasons. However, OCS fluxes provide evidence of a new stress response, new insight into the heterogeneity of the forest canopy and a new way to estimate the ecosystem stomatal conductance, without relying on the separation of soil evaporation from transpiration or measuring leaf temperatures. The observed behavior of OCS fluxes provides new challenges and opportunities for testing land-surface and carbon-cycle models.

carbonyl sulfide | carbon cycle | sulfur cycle | stomatal conductance | photosynthesis

INTRODUCTION

Carbonyl sulfide (OCS) is the most abundant sulfur gas in the atmosphere (1) and biogeochemical cycling of OCS affects both the stratosphere and troposphere. The tropospheric OCS mixing ratio is between 300 and 550 ppt (1) (parts per trillion; 10^{-12}; pmol mol^{-1}), decreasing sharply with altitude in the stratosphere (2). In times of low volcanic activity, the sulfur budget and aerosol loading of the stratosphere are largely controlled by transport and photo-oxidation of OCS from the troposphere (3). The processes regulating emission and uptake of OCS are important factors in determining how changes in climate and land cover may impact the stratospheric sulfate layer.

OCS sources are predominantly from the oceans (4), with smaller emissions from anthropogenic and terrestrial sources, such as wetlands and anoxic soils (e.g. 5, 6) and oxic soils during times of heat or drought stress (e.g. 7, 8). The largest sink for OCS is the terrestrial biosphere (1, 4, 9), with uptake by both oxic soils (e.g. 10) and vegetation (e.g. 11). Once OCS passes through the stomata of plants, consumption of OCS is controlled by carbonic anhydrase (CA), the same enzyme that hydrolyzes carbon dioxide (CO_2) in the first step of photosynthesis (12). CA catalyses the irreversible hydrolysis of OCS to H_2S and CO_2.

The similarities in the uptake pathways have led to the use of OCS fluxes as a means to estimate CO_2 uptake by photosynthesis (13-15). Net carbon uptake measured in the terrestrial biosphere (Net Ecosystem Exchange, NEE) is the combination of two large fluxes: photosynthesis (Gross Primary Productivity, GPP) and respiration (Ecosystem Respiration, R_{eco}). Using an accepted *standard method* (16), GPP is estimated from NEE by subtracting day-time ecosystem respiration (R_{eco}), which was itself extrapolated from the temperature dependence of night-time NEE (NEE $- R_{eco}$ = GPP). The uncertainty in the calculation of GPP could be reduced, and its ecological significance increased, by developing independent methods of calculation.

Initial OCS ecosystem flux estimations were made using flask sampling following by analysis via gas chromatography – mass spectrometry (GC-MS (13, 15), but these studies did not have sufficient resolution to examine daily or hourly controls on the OCS flux. Laser spectrometers have been developed in the past few years to enable direct, *in situ* measurement of OCS ecosystem fluxes by eddy covariance. Recently, short-term measurements of the OCS ecosystem flux above arid forests (17) and an agricultural field (8, 18) have been reported. In this paper we describe the factors controlling the hourly, daily, seasonal and annual fluxes of OCS in a forest ecosystem, using a year (2011) of high frequency, direct measurements at Harvard Forest, MA, USA. We report here on the seasonal cycle, the OCS response to environmental conditions and the total deposition flux of OCS throughout the year. We compare these fluxes to corresponding measurements of CO_2 flux and derived estimates of photosynthetic uptake of CO_2 and ecosystem respiration.

Significance

We describe the factors controlling the hourly, daily, seasonal and annual fluxes of carbonyl sulfide (OCS) in a forest ecosystem. Vegetation dominated daytime OCS uptake. Night-time fluxes accounted for 28% of the total annual uptake, with contributions from incompletely closed stomata and soils. Net OCS emission was observed at high temperatures in summer. Diurnal and seasonal variations in OCS flux do not have constant stoichiometry relative to the photosynthetic uptake of CO_2. Canopy OCS fluxes provide direct information on stomatal conductance and other photosynthetic related variables at the ecosystem scale. OCS can provide significant independent information on ecosystem processes, but an explicit model framework is required.

Reserved for Publication Footnotes

Seasonal Fluxes of OCS and CO$_2$ at Harvard Forest, 2011
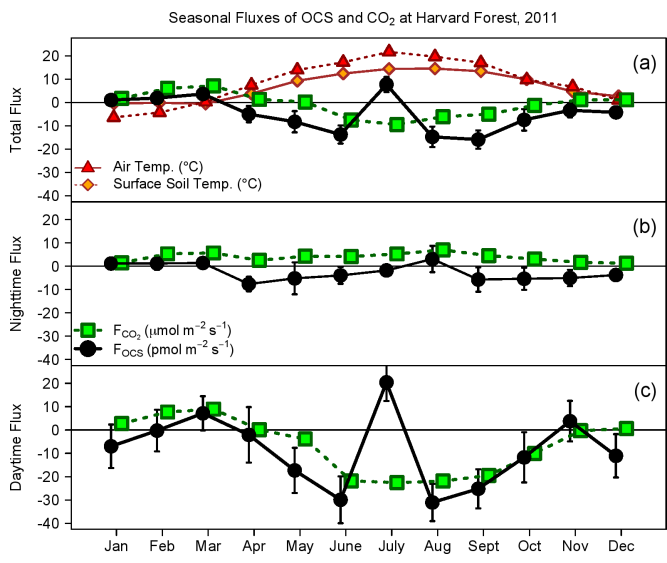
Fig. 1. Monthly mean OCS (F$_{OCS}$, pmol m^{-2} s^{-1}, black) and CO$_2$ (F$_{CO2}$, µmol m^{-2} s^{-1}, green squares) fluxes for 2011. u* > 0.17 m s^{-1} for all data. (a) Total OCS and CO$_2$ flux by month. Air temperature (red triangles, °C) and surface soil temperatures (orange diamonds, °C); CO$_2$ net flux includes changes in storage, but this is not required for OCS. (b) Night-time OCS (black) and CO$_2$ (green) flux (PAR < 40 µE m^{-2} s^{-1}) (c) Day-time OCS and CO$_2$ fluxes with PAR > 600 µE m^{-2} s^{-1}. Error bars indicate the 95% confidence intervals for all data within the month.

Results and Discussion

Details of the measurement method and deployment at the Environmental Measurement Site (EMS) flux tower at Harvard Forest are presented in the Methods and *Supporting Information*.

Seasonal Fluxes of OCS show strong vegetative uptake. Ecosystem fluxes of OCS (F$_{OCS}$) varied through the year with air and surface soil temperatures and showed complex behavior (Fig. 1, *Supporting Information*). The observed time series of OCS mixing ratios in 2011 followed the typical seasonal cycle measured previously at Harvard Forest (Fig. S1, (1)). Total net OCS flux for 2011 was -43.5 ± 0.5 gS ha^{-1} yr^{-1} (uptake from the atmosphere). Night-time uptake accounted for -12.3 ± 0.4 gS ha^{-1} yr^{-1}, ~28% of total uptake, peaking in spring and autumn (Fig. 1(b), *Supporting Information*).

As expected, the largest uptake fluxes were observed during summer (Fig. 1). OCS uptake started in April when conifer trees became active and the snowpack melted to expose the forest soil. Day-time OCS uptake increased through May and June in parallel with photosynthesis, marked by bud break of deciduous trees (May 5th) and sharply increased rates of sap flow (May 19th). This trend was unexpectedly interrupted by strong *emission* of OCS during midday hours in late July, when soil moisture was lowest and air temperatures the warmest of the year. As soil moisture gradually increased in August, day-time net OCS uptake resumed but net night-time OCS emission was observed (Fig. 1(b)). In September and October, the daily total and day-time OCS uptake flux decreased as air and soil temperatures decreased, while night-time OCS uptake resumed. Day-time OCS emissions were observed again in early November, during the senescence of red oak (*Quercus rubra*) leaves, cancelling the night-time uptake and resulting in a daily mean F$_{OCS}$ ~ 0. In December, low snowfall and above-freezing air and soil temperatures appeared to stimulate day-time OCS uptake greater than observed at night, possibly reflecting uptake of OCS by conifer trees.

Night-time OCS uptake. Night-time, light-independent, uptake of OCS is likely mediated by both soils and vegetation.

Soil fluxes are significant for both CO$_2$ and OCS, but have opposite signs: CO$_2$ is respired from soils, while OCS is generally taken up. Carbonic anhydrase is present in soil microorganisms (19) typical of oxic soils found at Harvard Forest. OCS is taken up by these microbes in oxic soils, albeit generally at a slower rate on the ecosystem scale than OCS uptake by vegetation (20). Hence, at times of net ecosystem CO$_2$ respiration, the deposition velocity of OCS relative to CO$_2$ (v$_{OCS}$:v$_{CO2}$) is negative (Table 1).

Nighttime transpiration through incompletely closed stomata has been observed in many tree species (21, 22) and night-time OCS uptake has been observed in deciduous and conifer forests during the growing season (23, 24). Maseyk et al [2014] (8) attributed ~29% of total OCS flux to night-time OCS uptake by vegetation, in that case winter wheat, with 1-6% due to soils at the peak of the growing season. The results of these short-term studies generally agree with our growing season results. However, the continued strong uptake of OCS from October through December (deposition velocity, v$_{OCS}$ = 0.9 - 0.3 cm s^{-1}) points to continuing OCS uptake after the decline in activity of the deciduous canopy, and implicating soil uptake as a large influence on the annual uptake. Persistent uptake by soils, and potentially conifers, may contribute to the strong vertical gradient in OCS mixing ratios observed over North America from October to December (1).

Separating vegetative and soil uptake of OCS and CO$_2$:
In order to separate the influence of soil and vegetative processes, we examined time periods when each process dominates: early December (soil uptake dominant), April/November (soil and conifer) and May-October (soil, conifer and deciduous trees).

In early December, deciduous leaves were absent and air temperatures were below freezing. Soil temperatures at Harvard Forest were 2.5°C higher than the 12 year average (2001-2012) all the way through October and November, encouraging microbial activity into the winter, even when air temperatures dropped below freezing. Our estimate for OCS uptake by active soils, -7.2 ± 3.4 pmol m^{-2} s^{-1}, compares well with the average soil flux measured in a creek area in Colorado (23) of -7 ± 2.6 pmol m^{-2} s^{-1} and is slightly greater uptake than the average OCS uptake by soil in a mixed pine and broad-leaf forest in China (25) of -4.8 ± 2.9 pmol m^{-2} s^{-1}. As expected with a soil sink, after the soils froze, the OCS flux was not significantly different from zero (Fig. S5).

Prior to the thaw in April, the mean OCS uptake flux was indistinguishable from zero. Once the soils thawed and conifer activity began, daytime uptake (F$_{OCS}$ = -18.8 ± 18.0 pmol m^{-2} s^{-1}) was greater than the nighttime OCS uptake (F$_{OCS}$ = -7.7 ± 5.4 pmol m^{-2} s^{-1}), suggesting daytime conifer leaf uptake of ~ -11 pmol m^{-2} s^{-1}. The April nighttime uptake is comparable to the early December daytime uptake, when air temperatures were below 4°C. At a flux tower (called the Hemlock tower and described in *Supporting Information*) located in a conifer stand 500 m from the primary EMS tower, peak uptake of CO$_2$ was observed in the April-June period. The conifer-related OCS uptake of -11 pmol m^{-2} s^{-1} observed at the EMS tower in April may be the upper limit of OCS uptake by conifer species. Future measurements of the seasonal cycle of the OCS flux in a conifer forest are required to examine this question. In November, measurements of sap flow rate (*Supporting Information*) show that the red oak trees activity was sharply diminished after November 13th. This date also marks the time total ecosystem OCS uptake became similar to the early December soil fluxes, with no statistical difference between daytime (F$_{OCS}$ = -6.0 ± 10.9 pmol m^{-2} s^{-1}) and nighttime (F$_{OCS}$ = -10.3 ± 7.6 pmol m^{-2} s^{-1}) OCS fluxes.

Ecosystem OCS flux dependence on wind direction. There is heterogeneity in the tree species distribution within the flux tower footprint (*Supporting Information*). In June, August and September, air arriving at the tower from the north-west (NW;

273
274
275
276
277
278
279
280
281
282
283
284
285
286
287
288
289
290
291
292
293
294
295
296
297
298
299
300
301
302
303
304
305
306
307
308
309
310
311
312
313
314
315
316
317
318
319
320
321
322
323
324
325
326
327
328
329
330
331
332
333
334
335
336
337
338
339
340

Table 1. : *Monthly mean of (1) Ecosystem deposition velocity of OCS (v_{OCS}), (2) Ratio of OCS to CO_2 deposition velocity (v_{OCS}/v_{CO2}), (3) Ratio of OCS to GPP deposition velocity ($v_{OCS}/GPP*$). ‡highlights period of net OCS emission. §The growing season mean (June-Sept. 2011) was calculated for v_{OCS}/v_{CO2} and $v_{OCS}/GPP*$ instead of an annual mean.*

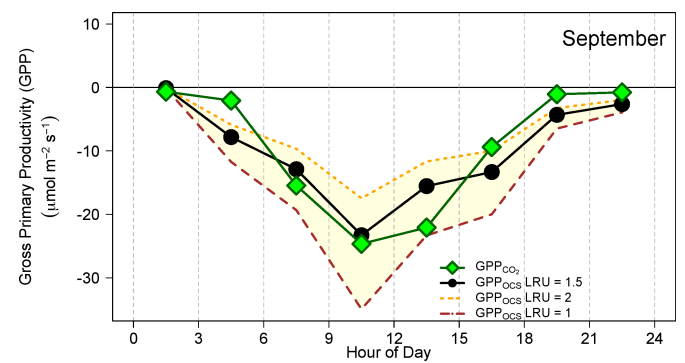|	Apr	May	Jun	Jul‡	Aug	Sep	Oct	Nov	Dec	Year
v_{OCS} (cm s⁻¹)	1.0	0.7	1.2	*-0.85*	1.4	1.6	0.9	0.3	0.5	**0.5**
v_{OCS}/v_{CO2}	-8.9	-8.9	1.5	*-1.1*	2.4	3.5	6.9	-2.9	-4.2	**-4.0**§
$v_{OCS}/GPP*$	5.5	1.8	0.8	*-0.6*	1.1	1.5	1.7	4.6	16.1	**1.8**§
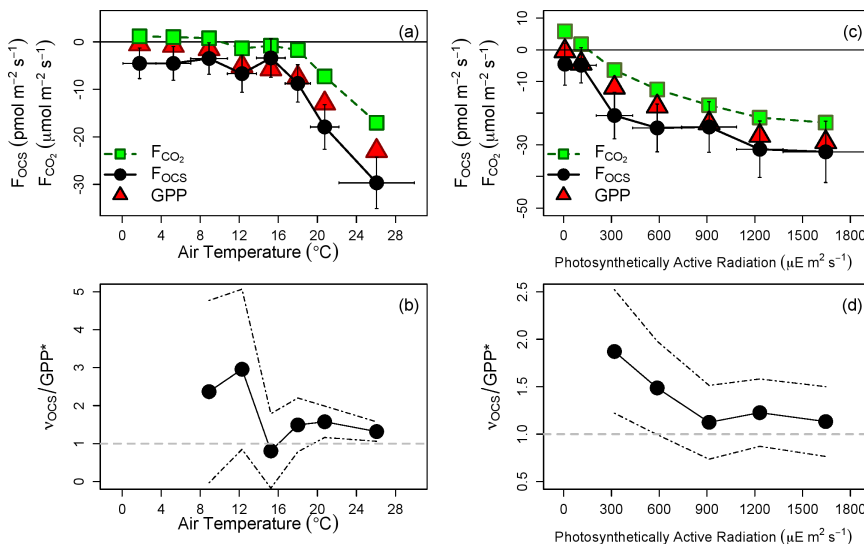
Fig. 2. The (left: a, b) Air temperature and (right: c, d) Photosynthetically Active Radiation (PAR) dependence of (a, c) OCS flux (F_{OCS}, pmol m⁻² s⁻¹, black circles), CO_2 flux (F_{CO2}, µmol m⁻² s⁻¹, green squares) and photosynthesis (calculated as GPP, µmol m⁻² s⁻¹, red triangles) and (b, d) $v_{OCS}/GPP*$. 95% CI are shown as black dashed lines. July data excluded. (a, b) include night-time data.
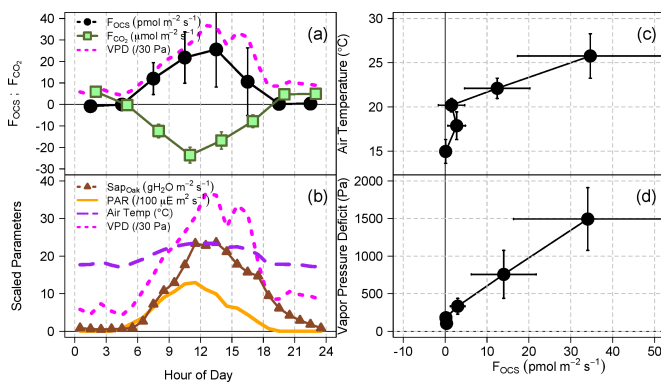
Fig. 3. Diel cycles of various fluxes and environmental parameters for July 20th-31st, 2011. **(a)** OCS (black circles; pmol m⁻² s⁻¹) and CO_2 fluxes (green squares; µmol m⁻² s⁻¹) and vapor pressure deficit (VPD, magenta dashed line; Pa/30) **(b)** Scaled parameters include sap flow rate of oak trees (brown triangles; gH2O m⁻² s⁻¹), photosynthetically active radiation (orange solid line; 10⁻⁸E m⁻² s⁻¹), air temperatures (purple long dashed line, °C), vapor pressure deficit (VPD, magenta dashed line; Pa/30) **(c)** Air temperature (°C) vs F_{OCS} (pmol m⁻² s⁻¹), with equalized air temperature data bins **(d)** Vapor pressure deficit (VPD) (Pa) vs F_{OCS} (pmol m⁻² s⁻¹), with equalized VPD data bins.

Fig. 4. GPP calculated directly from OCS fluxes (GPP_{OCS}, shaded area) with LRU values of 1 (brown long-dash line), 1.5 (black points) and 2 (orange dotted line) and indirectly extrapolated from night-time temperature dependent respiration (GPP_{CO2}, green diamonds) for September 2011.**Table 1:**Monthly mean of (1) Ecosystem deposition velocity of OCS (v_{OCS}), (2) Ratio of OCS to CO_2deposition velocity (v_{OCS}/v_{CO2}), (3) Ratio of OCS to GPP deposition velocity ($v_{OCS}/GPP*$). ‡highlights period of net OCS emission. §The growing season mean (June- Sept. 2011) was calculated for $v_{OCS}/v_{CO2}$and $v_{OCS}/GPP*$ instead of an annual mean.

mixed conifer and deciduous) sector in the daytime saw almost twice as much OCS uptake (NW F_{OCS} = -40.9 ± 8.2 pmol m⁻² s⁻¹) as air from the south-west (SW; deciduous dominated) sector (SW F_{OCS} = -23.5 ± 8.2 pmol m⁻² s⁻¹). Even though the daytime net CO_2 flux is the same in both wind directions, the increased daytime OCS uptake flux in air from the NW sector, combined with increased night-time ecosystem respiration (R_{eco}) from the

NW, suggests that the magnitude of the daytime R_{eco} and GPP is greater in air from the conifer dominated north-west sector.

Outside of July, a temporal trend was observed in the OCS flux in the SW sector, with OCS emission after noon in June (but with very few data points) and slightly depressed OCS uptake after noon in August (cancelled out by the large NW OCS uptake). Both of these periods appear to reflect an influence of

341
342
343
344
345
346
347
348
349
350
351
352
353
354
355
356
357
358
359
360
361
362
363
364
365
366
367
368
369
370
371
372
373
374
375
376
377
378
379
380
381
382
383
384
385
386
387
388
389
390
391
392
393
394
395
396
397
398
399
400
401
402
403
404
405
406
407
408

daytime OCS emission processes outside the period of measured net emission described below.

Deposition velocity of OCS relative to CO₂. Comparing the deposition velocity of OCS and CO_2 for various environmental conditions allows us to contrast the differing mechanisms involved in the vegetative uptake of each gas species. Both OCS and CO_2 diffuse from the atmosphere through stomata into leaves, where they are hydrolyzed by the light-independent enzyme carbonic anhydrase (CA). For OCS, the products are H_2S and CO_2, and the process is thought to be irreversible. In contrast, photosynthesis of CO_2 is a two-step process: diffusion into the leaves, reversible hydration by CA, then light-dependent and irreversible fixation by RuBisCo. Uptake of OCS does not require light but responds to light indirectly, via stomatal opening. The OCS flux is largely controlled by the series conductance of the stomata, and the mesophyll (cell walls and membranes) for diffusion of OCS from the air to the site of the CA reaction (4). Both of these conductances tend to be correlated with the amount of RuBisCo, and this probably explains the link between the light saturated rates of CO_2 and OCS uptake (4).

The ratio of the ecosystem deposition velocity of OCS (v_{OCS} (cm s⁻¹)) to that of CO_2 (v_{OCS}:v_{CO2}) showed strong dependence on air temperature (Fig. 2(a)) and photosynthetically active radiation (PAR) (Fig. 2(b)). We observed strong OCS uptake earlier in the day, which persisted later in the day, than net CO_2 uptake, where uptake has to offset respiration. This behavior was predicted by Goldan *et al [1988]* (11), and is observed here for the first time at the ecosystem scale (Fig. 2(c)). When temperatures rose above 16°C, net F_{CO2} changed from positive (respiration dominated) to negative (photosynthesis dominated). When the canopy was fully developed and leaves in the canopy were most active, uptake of both OCS and CO_2 were strongest, peaking at the highest temperatures, except for the anomalous period in July when OCS was emitted by leaves but CO_2 uptake continued (Table 1).

The ratio of the ecosystem deposition velocity of OCS to CO_2 (v_{OCS}:v_{CO2}) can be compared to the Ecosystem Relative Uptake (ERU) of OCS to CO_2 (1, 13, 14). The ERU calculated for aircraft-profile derived v_{OCS}:v_{CO2} (4.6 - 6.5 for the New England area in July-August 2004 (13)), were both higher than the v_{OCS}:v_{CO2} ratio calculated for the flux tower (4.6 for 2011). This difference is likely due to the larger non-vegetative sources of CO_2 (including anthropogenic) than OCS (marine, anthropogenic) in the wider region not present within the tower footprint. During summer months when photosynthesis was greatest (June-Sept, excl. July), the mean daily v_{OCS}:v_{CO2} ratio was 2.6 ± 0.7 and the mean daytime (8am-5pm EST) v_{OCS}:v_{CO2} ratio was 1.5 ± 0.3. The v_{OCS}:v_{CO2} ratio increased from August through October (Table 1).

In order to remove the influence of respiration on the v_{OCS}:v_{CO2} ratio we calculated the GPP of the forest normalized by the ambient CO_2 concentration (GPP* (cm s⁻¹)). Using the *standard method* described previously, GPP was estimated from NEE by subtracting day-time ecosystem respiration (R_{eco}), which was extrapolated from the temperature dependence of nighttime NEE (NEE − R_{eco} = GPP) (16). The v_{OCS}:GPP* ratio varied through the season, with a relatively high v_{OCS}:GPP* in May and October, (greater relative OCS uptake), decreasing to a (negative) minimum in July (due to OCS emission) (Table 1). The v_{OCS}:GPP* ratio generally decreased with air temperature (Fig. 2(b)). The mean v_{OCS}:GPP* ratio for temperatures above 14°C (i.e. times of full canopy) was 1.4 ± 0.3. The flux-weighted average for the year was 1.8 (Table 1). The mean v_{OCS}:GPP* ratio for higher temperatures includes both day and night values and therefore is lower than the mean values obtained at higher PAR values (Fig. 2(d)). v_{OCS}:GPP* is comparable to the leaf-scale v_{OCS}:v_{CO2}, also known as Leaf-scale Relative Uptake (LRU).

Recent work has identified a range of LRU values, including leaf-chamber studies that have measured LRU values of 1 − 4 (26) and 1.3 - 2.3 (23) for a variety of tree species, and a field study of wheat that measured LRU values of 0.9 - 1.9 for various light conditions (8). In our study, v_{OCS}:v_{GPP} for times of air temperatures 14-28°C and full light for the fully developed deciduous canopy was 1.4 ± 0.3, a value within the range of observed LRU values. However v_{OCS}:GPP* was not constant during the day, with the highest values at times of low light early and late in the day. These variations in LRU values are somewhat more complex than commonly assumed, but nevertheless can be well represented in simulations with a carbon-cycle model (Simple Biosphere Model, SiB) modified to include soil and canopy exchange of OCS (4) (*Methods*).

Emission of OCS. Both light-dependent and light-independent mechanisms contribute to the net OCS emissions from the ecosystem observed during 2011. Net emission of OCS was observed forest-wide (all wind directions), day and night, under the high air temperature (>30°C) conditions in late July and early August. Net OCS emission was also observed in air from the deciduous-dominated wind sector in late June and August, and during senescence in November. Figure 3 shows the diel cycle of OCS emission and CO_2 uptake for 11 days at the end of July (July 20th – July 31st) (F_{OCS} maximum = +22.7 ± 9.4 pmol m⁻² s⁻¹). Heat stress may have been a determining factor in the observed OCS emission, which was strongly enhanced at air temperatures above 21°C (Fig. 3 (c)), vapor pressure deficit (VPD) greater than 500 Pa (Fig. 3 (d)) and sap flow rates above 10 gH_2O m⁻¹ s⁻¹ (not shown). In the absence of OCS emission from the ecosystem, the expected day-time net OCS uptake due to hydrolysis by CA (based on June and August peak OCS ecosystem uptake) should be around -30 pmol m⁻² s⁻¹, and hence the *net* emission of +20 pmol m⁻² s⁻¹ in late July could correspond to a maximum *gross* emission by other mechanisms of 50 pmol m⁻² s⁻¹ at midday. A recent study reported OCS emission from temperature-stressed soils and senescent wheat at harvest-time (8, 18). However, the emission observed here occurred at temperatures much lower than in the wheat field study. Nighttime OCS emission peaked in August (Fig 1(b)), when CO_2 respiration was greatest, indicating a light-independent emission mechanism, possibly associated with decomposition.

Soil warming and nitrogen fertilization experiments have been conducted in plots to the SW of the tower from 2006 to present, including during 2011 (27, 28). These experiments use ammonium nitrate (NH_4NO_3) to fertilize 12 plots of size 3 x 3 m. The fertilizer contains trace levels of sulfur (approximately 0.002% sulfur as SO_4^-), which is equivalent to an application of 2.2 gS ha⁻¹ yr⁻¹, a less than 0.01% increase on the sulfur content of the soil. The periods of OCS emissions were not found to correlate with the application of the fertilizer. While we cannot discount the possibility of an OCS artifact from the fertilizer, we suspect that the small area involved and the low levels of sulfur application are too small to contribute to the observed OCS signal. Nitrogen fertilization experiments also found increased OCS emission from soils (29) but we do not see a correlation with soil temperature and the related increase in microbial activity. It is possible that the sulfur present in the soils at Harvard Forest, like the soils of the wheat fields in Oklahoma (8), is a source of OCS through some unknown biophysical mechanism.

In early November OCS emission fluxes of ~5pmol m⁻² s⁻¹ were observed briefly during the leaf senescence of the red oak trees. It is possible this emission occurred through a process similar to that observed during wheat senescence in Oklahoma (8). High surface soil temperatures were also implicated as a source of OCS in that study. However the soil temperature at

Harvard Forest never reached the high temperatures observed in Oklahoma as the canopy shielded the forest floor from direct light, and there is no correlation of OCS emission with soil temperature at Harvard Forest in November. Therefore, we propose that the source of OCS may have been within the senescent canopy or from freshly fallen leaves in the litter layer on the forest floor.

OCS fluxes in the forest ecosystem. Ecosystem scale fluxes of OCS have been adopted as a means to directly determine the photosynthetic uptake of carbon in the biosphere, independently of soil and plant respiration (13, 14, 17). However, for this approach to work as proposed, a number of requirements must be met, many of which are not realized year-round at Harvard Forest. These conditions include: 1) F_{OCS} should be unidirectional (i.e. no OCS emission). *We observed net OCS emission at times of ecosystem stress.* 2) Night-time uptake of OCS should be negligible or relatively constant and quantifiable. *We found night-time uptake varies throughout the year and accounts for $\sim$28% of the annual OCS uptake.* 3) The leaf-scale relative uptake (LRU) of OCS/CO_2 for the ecosystem type should be known. Recent work has identified a range of LRU values, including leaf-chamber studies that have measured LRU values of $1 - 4$ (26) and 1.3 - 2.3 (23) for a variety of tree species, and a field study of wheat that measured LRU values of 0.9 - 1.9 for various light conditions (8). *Our study shows that the ecosystem v_{OCS}:GPP*, which can be related to LRU (Supporting Information), is not constant. Values vary within the reported range of LRU values, provided that environmental conditions are restricted to air temperatures between 14°C and 28°C (Fig. 3(b)), PAR > 600 μE m^{-2} s^{-1} (Fig 3(d)), times of full canopy and average soil moisture.*

In view of these limitations, we tested the applicability of OCS for the approximation of GPP (GPP$_{OCS}$) during ideal conditions (high illumination with moderate temperatures and soil moisture) in September 2011 (LRU = v_{OCS}:GPP* = 1.5 ± 0.5, Fig. 4). The total daily sum of GPP$_{OCS}$ and GPP$_{CO2}$ agree to within 3.5% for an LRU of 1.5, but the agreement is tightly coupled to the range of LRU values used (8, 17). Changing the LRU from 2 to 1 resulted in a 29% underestimation becoming a 36% overestimation (Fig. 4). GPP$_{OCS}$ extends through more of the day than GPP$_{CO2}$, (earlier morning and later evening uptake), highlighting the differing light dependent uptake pathways of OCS and CO_2 discussed earlier. We conclude that OCS fluxes are related to GPP at times of greatest CO_2 uptake, but this linkage breaks down under limiting light and is complicated by other uptake and production processes. Despite these complications, the OCS fluxes calculated using the SiB model (4) generally matched the observed fluxes well, and a more detailed modeling study is planned.

Measurements of ecosystem OCS fluxes show promise in providing a new means to estimate stomatal conductance on the ecosystem scale. Stomatal conductance at our site was calculated using the Ball-Berry equation in the SiB model and an explicit representation of OCS fluxes (4) (*Methods*). We found a strong linear correlation between the observed ecosystem OCS fluxes and both the calculated stomatal conductance ($r^2 = 0.84$) and the simulated OCS fluxes ($r^2 = 0.63$) for the eddy flux data from August to October 2011. Previous laboratory studies had proposed that OCS fluxes should scale directly with stomatal conductance (30, 31), however this is the first evidence of this relationship in a forest ecosystem, and nocturnal uptake of OCS by the canopy provides strong evidence for incomplete stomatal closure at night. Using the OCS flux as a means to measure the stomatal conductance independently of the water vapor flux would be a major advance in our capability to assess ecosystem response to environmental forcing.

CONCLUSIONS AND IMPLICATIONS

Ecosystem fluxes of carbonyl sulfide (OCS) were measured at Harvard Forest, MA throughout 2011. The overall net uptake of OCS totaled -43.5 ± 0.5 gS ha^{-1} yr^{-1} in the forest ecosystem, with 28% of uptake occurring at night, which was attributed to both soil uptake and vegetative uptake through incompletely closed stomata. The flux of OCS was found to be bidirectional, with net emission during hotter conditions, and when vegetation senesced. Air temperatures at Harvard Forest have warmed 1.5°C over the past 50 years (32, 33) with increasingly large interannual variability, and drought and heat stress events are expected to increase in frequency (34). Our results suggest that the balance of OCS uptake versus emission may change in terrestrial ecosystems with an increasing number of events that induce stress in forests, leading to changes in the global OCS budget. The leaf scale relative uptake of OCS:CO_2 was found to vary diurnally with high values at dawn and dusk. The ecosystem OCS flux is not a direct measure of photosynthesis, with many of the assumptions in this simple method found to be invalid for different times of our year-round observation. However, the addition of OCS flux to the conventional suite of eddy covariance measurements provided new information on stomatal behavior, canopy and soil heterogeneity, soil processes and stress responses. Matching the contrasting behavior of CO_2 and OCS fluxes could present new challenges for carbon cycle models at the ecosystem-scale, and such models could be useful in interpreting the large variation in OCS concentration observed in the atmosphere at regional- and continental-scales.

METHODS

A Tunable Infra-red Laser Direct Absorption Spectrometer (TILDAS, Aerodyne Research Inc.) was used to measure atmospheric mixing ratios and derive gradients and fluxes of carbonyl sulfide and water vapor at 2048.495 cm^{-1} and 2048.649 cm^{-1} respectively. Mixing ratios of OCS and H_2O at a frequency of 4 Hz for eddy covariance flux (eF$_{OCS}$; August 2011 – December 2011) or 1 Hz for gradient-flux (gF$_{OCS}$; January 2011 – August 2011) were calculated using TDL Wintel software (Aerodyne Research Inc.). The 1σ instrument precision was typically 14 ppt at 4 Hz, averaging down to <1 ppt at 60 s. The sensor is a further development of earlier instruments (35-38). More details about the measurement technique and associated instrumental tests and the theory behind the flux calculations are provided in *Supplementary Information*. Tests were conducted to ensure continuity of measurement techniques. A comparison of the OCS mixing ratios (TILDAS) observed at the same time as NOAA flask samples is shown in Fig. S1.

Measurements were made at the Environmental Measurement Site (EMS) at Harvard Forest, Petersham, MA (42.54°N, 72.17°W, elevation 340 m). The CO_2 flux has been measured at this Long Term Ecological Research (LTER) site since 1990 (39). Details about the site, environmental conditions and ancillary measurements during the study period are described in the *Supplementary Information*. Environmental conditions for the study were typical of New England. Up to 75 cm of snow accumulated between January and April in 2011. Air temperatures ranged from -28°C in January to 35°C in July. At Harvard Forest, conifer trees are generally not active when air temperatures are consistently below freezing (40). The CO_2 flux from soil respiration depends mainly on microbial activity and CO_2 diffused through the snowpack, with increased exchange from wind pumping. Microbial activity continued through the winter as the soil temperatures were partially shielded from the low air temperatures by the insulating snow pack (41) before the frost depth extended down to 10cm into the soil in early March. Bud break was observed for deciduous species around May 5th and senescence began late in October. Prolonged power loss resulted from damage to power lines and damage to electronic equipment due to lightning on May 28th. As no OCS fluxes were measured during the first two weeks of May and again the first two weeks of June, the mean uptake for both May and June was based only on measurements during the last half of each month. There was less than 60 mm precipitation during June and July and this precipitation was concentrated into four short events. Prolonged high temperatures (> 30°C) affected the site in mid-July, resulting in low soil moisture in the area. Storms arrived in early August, bringing prolonged and heavy precipitation and increasing soil moisture. Hurricane Irene on August 28th caused extensive flooding in the region. October was unseasonably warm and leaves were still on trees when a snow-storm on October 29th brought almost 50 cm of snow to the area, again resulting in a brief power cut at the site and flooding in the area on thaw. These large moisture events resulted in greater cumulative precipitation for 2011 (1635 mm) than the 10-year average for the site (1226 mm), even though soils were anomalously dry in July.

OCS fluxes derived during times of low turbulence ($u* < 0.17$ m s^{-1}) and during periods of precipitation were removed (16), leaving valid data covering 34% of the 30 minute periods over the entire year, slightly less than the 45% reported by *Urbanski et al., [2007]* as the mean valid CO_2 flux data points for the years 1992-2004. The valid data were uniformly distributed over the year, and every hour for each composite month throughout the year had valid OCS flux data, allowing the yearly flux of OCS to be calculated for 2011 as -136 μmol m^{-2} yr^{-1}, corresponding to a net uptake of -43.5 ± 0.5 gS (as OCS) ha^{-1} yr^{-1} or -16.3 ± 0.1 gC (as OCS) ha^{-1} yr^{-1} by the biosphere. The total CO_2 flux for the year, selected from times of valid OCS fluxes, was -22.6 mol m^{-2} yr^{-1} or -2.7 MgC ha^{-1} yr^{-1} for 2011. This value is within the observed range of -1.0 to -4.7 Mg C ha^{-1} yr^{-1} for the years 1992-2004 (42). Overall the OCS fluxes had a greater relative uncertainty than fluxes of CO_2, reflecting a combination of both a less precise measurement of the OCS flux (the gradient-flux calculated OCS flux has more uncertainty than the eddy covariance calculated OCS flux) and more variability of the actual day-time OCS fluxes.

The Simple Biosphere Model (SiB) version 3, adapted to include OCS, was run using 2011 meteorology data from Harvard Forest. SiB is a process-oriented enzyme-kinetic model that utilizes Michaelis-Menten kinetics following Farquhar et al. (1980) (43). SiB links stomatal conductance (both C3 and C4) to the energy budget (44, 45) and incorporates satellite-specified phenology (46). Stomatal conductance, determined by the Ball-Berry equa-tion (47), has a direct dependence on relative humidity and CO_2 concentration, and indirect dependence on soil water, temperature, light, and humidity through the assimilation term. Both leaf and soil uptake of OCS are explicitly represented in SiB (4) independently but in the same mechanistic framework as CO_2. The agreement between the observed and calculated OCS outside of the net emission in July is excellent (Figure S6). Work is underway to understand the differences observed in night-time data (Fig. S6 (a)) and to include emission processes in SiB.

1. Montzka SA et al. (2007) On the global distribution, seasonality, and budget of atmospheric carbonyl sulfide (COS) and some similarities to CO2. *Journal of Geophysical Research* 112:D09302.
2. Barkley MP, Palmer PI, Boone CD, Bernath PF, Suntharalingam P (2008) Global distributions of carbonyl sulfide in the upper troposphere and stratosphere. *Geophys Res Lett* 35:L14810.
3. Brühl C, Lelieveld J, Crutzen PJ, Tost H (2012) The role of carbonyl sulphide as a source of stratospheric sulphate aerosol and its impact on climate. *Atmos Chem Phys* 12:1239–1253.
4. Berry J et al. (2013) A coupled model of the global cycles of carbonyl sulfide and CO2: A possible new window on the carbon cycle. *J Geophys Res Biogeosci* 118:1–11.
5. Li X, Liu J, Yang J (2006) Variation of H2S and COS emission fluxes from Calamagrostis angustifolia Wetlands in Sanjiang Plain, Northeast China. *Atmospheric Environment* 40:6303–6312.
6. Whelan ME, Min D-H, Rhew RC (2013) Salt marsh vegetation as a carbonyl sulfide (COS) source to the atmosphere. *Atmospheric Environment* 73:131–137.
7. Liu J et al. (2010) Exchange of carbonyl sulfide(COS) between the atmosphere and various soils in China. *Biogeosciences* 7:753–762.
8. Maseyk K et al. (2014) Sources and sinks of carbonyl sulfide in an agricultural field in the Southern Great Plains. *Proceedings of the National Academy of Sciences*.
9. Kettle AJ (2002) Global budget of atmospheric carbonyl sulfide: Temporal and spatial variations of the dominant sources and sinks. *Journal of Geophysical Research* 107.
10. Kuhn U et al. (1999) Carbonyl sulfide exchange on an ecosystem scale: soil represents a dominant sink for atmospheric COS. *Atmospheric Environment* 33:995–1008.
11. Goldan PD, Fall R, Kuster WC, Fehsenfeld FC (1988) Uptake of COS by Growing Vegetation: A Major Tropospheric Sink. *Journal of Geophysical Research* 93:14186–14192.
12. Protoschill-Krebs G, Wilhelm C, Kesselmeier J (1996) Consumption of carbonyl sulphide (COS) by higher plant carbonic anhydrase (CA). *Atmospheric Environment* 30:3151–3156.
13. Campbell JE et al. (2008) Photosynthetic Control of Atmospheric Carbonyl Sulfide During the Growing Season. *Science* 322:1085–1088.
14. Sandoval-Soto L et al. (2005) Global uptake of carbonyl sulfide (COS) by terrestrial vegetation: Estimates corrected for deposition velocities normalized to the uptake of carbon dioxide (CO2). *Biogeosciences* 2:125–132.
15. Blonquist JM Jr. et al. (2011) The potential of carbonyl sulfide as a proxy for gross primary production at flux tower sites. *Journal of Geophysical Research* 116:G04019.
16. Goulden ML, Munger JW, Fan S-M, Daube BC, Wofsy SC (1996) Measurements of carbon sequestration by long-term eddy covariance: methods and a critical evaluation of accuracy. *Global Change Biology* 2:169–182.
17. Asaf D et al. (2013) Ecosystem photosynthesis inferred from measurements of carbonyl sulphide flux. *Nature Geosci* 6:186–190.
18. Billesbach DP et al. (2014) Growing season eddy covariance measurements of carbonyl sulfide and CO2 fluxes: COS and CO2 relationships in Southern Great Plains winter wheat. *Agricultural and Forest Meteorology* 184:48–55.
19. Kato H, Saito M, Nagahata Y, Katayama Y (2007) Degradation of ambient carbonyl sulfide by Mycobacterium spp. in soil. *Microbiology* 154:249–255.
20. Van Diest H, Kesselmeier J (2008) Soil atmosphere exchange of carbonyl sulfide (COS) regulated by diffusivity depending on water-filled pore space. *Biogeosciences* 5:475–483.
21. Caird MA, Richards JH, Donovan LA (2006) Nighttime Stomatal Conductance and Transpiration in C3 and C4 Plants. *Plant Physiol* 143:4–10.
22. Daley MJ, Phillips NG (2006) Interspecific variation in nighttime transpiration and stomatal conductance in a mixed New England deciduous forest. *Tree Physiology* 26:411–419.
23. Berkelhammer M et al. (2014) Constraining surface carbon fluxes using in situ measurements of carbonyl sulfide and carbon dioxide. *Global Biogeochem Cycles* 28:161–179.
24. White M et al. (2010) Carbonyl sulfide exchange in a temperate loblolly pine forest grown under ambient and elevated CO2. *Atmos Chem Phys* 10:547–561.
25. Yi Z et al. (2007) Soil uptake of carbonyl sulfide in subtropical forests with different successional stages in south China. *Journal of Geophysical Research* 112:D08302.
26. Stimler K, Montzka SA, Berry JA, Rudich Y, Yakir D (2010) Relationships between carbonyl sulfide (COS) and CO2 during leaf gas exchange. *New Phytologist* 186:869–878.
27. Contosta AR, Frey SD, Cooper AB (2011) Seasonal dynamics of soil respiration and N mineralization in chronically warmed and fertilized soils. *Ecosphere* 2:art36.
28. Contosta AR, Frey SD, Ollinger SV, Cooper AB (2012) Soil respiration does not acclimatize to warmer temperatures when modeled over seasonal timescales. *Biogeochemistry* 112:555–570.
29. Mellillo JM, Steudler PA (1989) The effect of nitrogen fertilization on the COS and CS2 emissions from temperature forest soils. *J Atmos Chem* 9:411–417.
30. Seibt U, Kesselmeier J, Sandoval-Soto L, Kuhn U, Berry JA (2010) A kinetic analysis of leaf uptake of COS and its relation to transpiration, photosynthesis and carbon isotope fractionation. *Biogeosciences* 7:333–341.
31. Stimler K, Berry J, Yakir D (2012) Effects of Carbonyl Sulfide and Carbonic Anhydrase on Stomatal Conductance. *Plant Physiol* 158:524–530.
32. Boose E, Gould E Shaler Meteorological Station at Harvard Forest 1964-2002.
33. Boose E Fisher Meteorological Station at Harvard Forest since 2001.
34. Diffenbaugh SN, Scherer M (2013) Likelihood of July 2012 U.S. temperatures in pre-industrial and current forcing regimes [in "Explaining Extreme Events of 2012 from a Climate Perspective"]. *Bulletin of the American Meteorological Society* 94:S6–S9.
35. Nelson DD, McManus JB, Urbanski S, Herndon S, Zahniser MS (2004) High precision measurements of atmospheric nitrous oxide and methane using thermoelectrically cooled mid-infrared quantum cascade lasers and detectors. *Spectrochimica Acta Part A-Molecular and Biomolecular Spectroscopy* 60:3325–3335.
36. McManus JB et al. (2010) Application of quantum cascade lasers to high-precision atmospheric trace gas measurements. *Opt Eng* 49:111124.
37. Stimler K, Nelson DD, Yakir D (2009) High precision measurements of atmospheric concentrations and plant exchange rates of carbonyl sulfide using mid-IR quantum cascade laser. *Global Change Biology*.
38. Commane R et al. (2013) Carbonyl sulfide in the planetary boundary layer: Coastal and continental influences. *J Geophys Res-Atmos* 118:1–9.
39. Urbanski S et al. (2007) Factors controlling CO2 exchange on timescales from hourly to decadal at Harvard Forest. *Journal of Geophysical Research* 112.
40. Hadley JL (2000) Effect of Daily Minimum Temperature on Photosynthesis in Eastern Hemlock (Tsuga canadensis L.) in Autumn and Winter. *Arctic, Antarctic, and Alpine Research* 32:368.
41. Sharratt BS, Baker DG, Wall DB, Skaggs RH, Ruschy DL (1992) Snow depth required for near steady-state soil temperatures. *Agricultural and Forest Meteorology* 57:243–251.
42. Keenan TF et al. (2013) Increase in forest water-use efficiency as atmospheric carbon dioxide concentrations rise. *Nature* 499:324–327.
43. Farquhar GD, Caemmerer von SV, Berry JA (1980) A biochemical model of photosynthetic CO2 assimilation in leaves of C3 species. *Planta* 149:78–90.
44. Collatz GJ, Ribas-Carbo M, Berry JA (1992) Coupled Photosynthesis-Stomatal Conductance Model for Leaves of C4 Plants. *Aust J Plant Physio* 19:519.
45. Collatz GJ, Ball JT, Grivet C, Berry JA (1991) Physiological and environmental regulation of stomatal conductance, photosynthesis and transpiration: a model that includes a laminar boundary layer. *Agricultural and Forest Meteorology* 54:107–136.
46. Sellers PJ et al. (1996) A Revised Land Surface Parameterization (SiB2) for Atmospheric GCMS. Part I: Model Formulation. *Journal of Climate* 9:676–705.
47. Ball JT, Woodrow IE, Berry JA (1987) in *Progress in photosynthesis research* (Springer Netherlands, Dordrecht), pp 221–224.

SUPPLEMENTARY MATERIAL

S1 Technical Details

S1.1 INSTRUMENT DESCRIPTION

A Tunable Infra-red Laser Direct Absorption Spectrometer (TILDAS, Aerodyne Research Inc.) was used to measure atmospheric mixing ratios and derive gradients and fluxes of carbonyl sulfide and water vapor at 2048.495 cm^{-1} and 2048.649 cm^{-1} respectively. *There were no CO_2 absorption lines in the spectral range of this laser.* Mixing ratios of OCS and H_2O at a frequency of 4 Hz (eddy flux) or 1 Hz (gradient-flux) were calculated using TDL Wintel software (Aerodyne Research Inc.). A background spectrum (30 s duration) was obtained every 10 minutes, and interpolated and subtracted from the sample spectra, in order to account for any temporal changes in instrument response. A diaphragm pump was used for gradient-flux measurements, which resulted in a flow rate of ~3 slm and cell response time of 15 s (90% response time). *The first 60 s at each level were discarded to allow for equilibration of water vapor.* The 1σ instrumental precision was 5 pptv (pmol mol^{-1}) in 1 s averaging down to 0.9 pptv at 100 s. During eddy-flux measurements, a TriScroll 600 slm pump resulted in a flow rate of 12 slm through the cell and a response time of 1 s. The 1σ instrument precision was typically 14 pptv at 4 Hz, likewise averaging down to <1 pptv at 60 s. The sensor is a further development of previous work (1-5). The instrument was an early version of the TILDAS instrument using a 210 m absorption cell in a thermally isolated plastic box used outside previously at Harvard Forest for the measurement of nitric acid and at a fen in New Hampshire for the measurement of methane isotope fluxes (6). Further instrumental developments lead to the instrument used in recent studies (7, 8).

The combined water vapor dilution and pressure broadening correction factor was 1.27 at this wavelength, which, if not corrected, could have caused an underestimation of 7 pptv (in 400 pptv) OCS for 14 ppth (mmol mol^{-1}) water vapor. This correction has been applied to the dataset. A NOAA-calibrated cylinder of OCS in air was regularly added to the gradient-flux setup (flow rate ~3 slm (standard liters per minute), however the high flow rate of the eddy flux method (~12 slm from August 4th) made frequent overblowing the inlet with a constant flow difficult and expensive. Instead the regular additions of OCS-free air for the null spectra were used to determine the temporal variations in the instrument stability, with less frequent addition of the calibration gas. These calibrations were independent of the NOAA flask samples described below.

Figure S1 shows a time series of OCS measured by the TILDAS (30 minute average) and OCS measured in weekly/fortnightly paired flask samples analysed by gas chromatography with mass spectrometric detection at NOAA (update of measurements from Montzka *et al.*, [2007] (9)). Most flask samples were collected at mid-day over a few minutes, after extensive flushing. The TILDAS measurements show short-term variability, often greatest outside of mid-day, that cannot be observed by the flasks. However, when the TILDAS data is averaged for the time periods around the flask sampling time (grey circles in Fig. S1), both measurements track well.

S1.2 CALCULATION OF OCS FLUXES

Two methods were used to calculate the canopy scale flux of OCS (F_{OCS}) at Harvard Forest. The gradient – flux method was used between January 2011 and early August 2011, followed by the eddy covariance method, which continued until the end of the year.

S1.2.1 Gradient – Flux Method

The micrometeorological gradient – flux method, also known as the modified Bowen ratio method (10), is based on the assumption of trace-gas similarity between OCS and, in our measurements, H_2O to calculate the flux of OCS, gF_{OCS} (pmol m^{-2} s^{-1}):

$$gF_{OCS} = F_{H_2O} \; gOCS / gH_2O \qquad \textbf{(S1)}$$

where gOCS (pmol mol^{-1} m^{-1}), gH$_2$O (mmol mol^{-1} m^{-1}), are the vertical concentration gradients of OCS and H_2O respectively measured simultaneously by the TILDAS at two heights (29.5 m and 24.1 m):

$$gX = [X]_{29.5m} - [X]_{24.1m} / (29.5 - 24.1) \qquad \textbf{(S2)}$$

and the water vapor flux F_{H_2O} is measured directly by eddy covariance at the EMS tower using a infra-red gas analyzer (IRGA, Li-COR 6262 (11)). The nominal TILDAS water vapor mixing ratios were 22% higher than the calibrated water vapor mixing ratios measured by the IRGA. The water vapor observed by the TILDAS was based on spectroscopic parameters, and was not externally calibrated, so this correction was applied to the TILDAS water vapor mixing ratios prior to calculation of the gradient – flux. *The gradient flux method has been used successfully at Harvard Forest previously to measure fluxes of hydrogen* {Meredith:2014hn}*, non methane hydrocarbons (NMHCs)*{Goldstein:1995vu, Goldstein:1996vi} *and isoprene* {Goldstein:1998wv}*. In each of these studies, the use of CO₂, H₂O and air temperature produced similar fluxes throughout the year with*

varying precision and accuracy. These methods were further validated when McKinney et al (2010) found similar fluxes of isoprene using disjunct eddy covariance method {McKinney:2011jt}. *Particularly relevant to the study here, Meredith et al. (2014) found that the gradient – flux method using either H_2O or CO_2 was valid throughout 2011* {Meredith:2014hn}.

The OCS flux could not be calculated for 23% of the OCS measurements made during the May-August 2011 sampling period. This was due to a combination of rain events (when no water vapor flux was calculated) and unrealistic water vapor mixing ratios (ΔH_2O outside the 95% quantiles of the total data), which resulted in equally unrealistic OCS fluxes. Figure S2 shows the diel cycle of the measurements of (a) OCS gradient and (b) H_2O gradient, (c) the H_2O flux measured by eddy flux, and (d) the calculated OCS flux using the gradient – flux method for June 14th, 2011. The CO_2 flux measured by eddy covariance (e) is included for comparison. Negative fluxes indicate loss from the atmosphere and uptake by the biosphere.

The overall uncertainty of the gradient – flux method was calculated for each point as the root-mean-square of the 95% confidence intervals of the gradient measurements (gOCS and gH_2O) and the mean error of the eddy covariance calculated water vapor (15% (11)). As the instrument is optimized to OCS detection, the error in the water vapor gradient measurement, combined with the standard deviation of the water vapor mixing ratio within a 30-minute period, dominated the overall uncertainty. For the June-July period, the uncertainty in absolute fluxes ranged from 0.05 pmol m^{-2} s^{-1} to 20 pmol m^{-2} s^{-1} on rare occasions with a median of 0.43 pmol m^{-2} s^{-1}. For example, as shown in Figure S2, this uncertainty reaches a maximum of 5.7 pmol m^{-2} s^{-1} for an OCS flux of 1.1 pmol m^{-2} s^{-1} on June 14th 2011.

For the gradient-flux method, ambient air was alternatively sampled from the tower heights of 29.5 m and 24.1 m using *40m of* 3/8" (OD; 0.95 cm) Synflex ® tubing. Teflon particle filters (pore size 5 µm) at the inlet of each sampling line were changed every 2-4 weeks to prevent artificial production of OCS on chemically aged or dirty surfaces (See Section S1.2.4 below). *These filters resulted in a pressure drop through the tubing, which reduced the effects of adsorption/desorption on the tubing. The black synflex tubing also reduced any sunlight affects on the sample.* The air in each sampling tube was tested after each background (10 or 30 minute interval) to ensure no *in situ* production of OCS (short-lived increase in OCS). The materials in the instrument were carefully chosen to minimize

any artifacts during sampling: clean Teflon filters, Synflex tubing, stainless steel solenoid valves and the glass sampling cell were not found to scavenge or emit OCS. No pump was used upstream of sampling to prevent contamination of the sample gas. Some initial measurements were made at 25 m and 1 m during the winter 2010-2011. The calculated fluxes for this winter 2011 period agreed with eddy fluxes for winter 2012, so these early data have been included in the seasonal cycle of F_{OCS}. For eddy covariance flux measurements, only the 29.5 m inlet was used.

S1.2.2 Eddy Covariance Method

The eddy covariance fluxes of OCS (eF_{OCS}) and H_2O (eF_{H_2O}) were calculated from high frequency (4Hz) measurements of OCS and H_2O made by the TILDAS at 29.5 m. After subtracting a block average for the interval, the covariance of the residual of the vertical wind velocity (w') and concentration (OCS' or H_2O') for each 30 minute interval was calculated as in Goulden *et al,.* [1996] (13)*,* e.g.

$$F_{OCS} = \overline{w'OCS'} \qquad eF_{OCS} = w'OCS' ; \qquad eF_{H_2O} = w'H_2O' \quad \textbf{(S3)}$$

The instrument synchronization time lag was determined by maximizing the correlation between w' and H_2O'. This lag also accounted for differences in computer clock times between the sonic and OCS data systems, which increased gradually after each synchronization reset (daily). The flux is rotated to the plane where the mean vertical wind is zero (14). The calibrated IRGA water vapor fluxes were used for all analysis. Accurate fluxes can be calculated even though high frequency noise limits the precision of the OCS concentration at short times, because the noise is not correlated with vertical wind velocity. The error in the eddy covariance was determined by calculating the root mean squared combination of observed covariance for periods ± 25 s from the lag time. This resulted in a mean standard error in the eddy covariance calculated OCS flux of 14%.

S1.2.3 Gradient-Flux and Eddy covariance comparison

Both gradient measurements and eddy flux measurements were made for a limited time period: 6 – 12 August 2011, when additional measurements were made at a height of 24.1 m for 120s every 30 minutes. This shorter sampling period at 24.1 m resulted in a greater error in the gradient-flux (gF_{OCS}) for this period (12). In a comparison of the two methods, the composite diel cycle (2 hourly bins) of gF_{OCS} (Figure S3 black circles) and eF_{OCS} (Figure S3 red boxes) for periods of common measurements showed similar behavior but

with slightly more variance in gF_{OCS}, as expected. The overall trend through the composite day compares well for both methods, with no statistical difference between the daily mean flux calculated by either method: daily mean OCS uptake of -8.6 (± 6.2; 95% CI) pmol m^{-2} s^{-1} for gF_{OCS} and -9.6 (± 4.4) pmol m^{-2} s^{-1} eF_{OCS}. The gradient-flux of OCS underestimates the total daily flux (gF_{OCS} = -174 pmol m^{-2} s^{-1}) by 7% compared to the eddy flux (eF_{OCS} = -187 pmol m^{-2} s^{-1}). The signs and the diel patterns of the flux are consistent for both methods, except during transition periods near sunrise and sunset when fluxes, especially the water vapor flux used to calculate gF_{OCS}, are small and neither method is reliable.

S1.2.5 OCS Storage

The actual net uptake or emission of a trace gas by the ecosystem is the observed vertical flux plus any accumulation (or depletion) in the canopy space below the flux sensor (storage term). For CO_2, the storage term is significant compared to the vertical flux, especially around dawn and dusk transitions - disregarding non-ideal conditions with significant horizontal advective fluxes. Although the storage term sums to nearly 0 over a daily interval, it must be included in order to interpret net CO_2 exchange on sub-daily intervals. During summer 2012 (and when large CO_2 storage values were calculated), storage of OCS calculated from OCS profile measurements were negligible. The physical process that leads to storage should not change from year to year so the results from 2012 should be applicable to 2011. Therefore storage has not been included ~~been ignored~~ in the OCS flux results that we report here.

S1.3 ARTIFICIAL OCS PRODUCTION

Heterogeneous production of OCS on the surface of the contaminated Teflon filters was observed over 5 days after sampling an anthropogenically-influenced airmass in February 2011, as unsafe climbing conditions prevented immediate replacement of the filter, which had been in place since late December. This OCS production was observed as large, short-lived pulses of OCS (up to 800 pptv) when sampling the line (and contaminated filter) after zero air background measurements. However, no evidence of OCS production from filter contamination was observed during the summer emission period described in the main text. Airmass trajectories for this February event indicate that the air was influenced by high sulfur emission from the copper and nickel smelters in Sudbury, Ontario, Canada, and SO_2 mixing ratios of greater than 60 ppbv were observed in the same airmass

at a site 60 miles east of Harvard Forest (Aerodyne Research, Billerica, MA) on the same day. OCS dissolves, but is not hydrolyzed, in acidic water. Belviso and co-workers measured supersaturated OCS in acidic rainwaters in France and suggested an *in situ* production of OCS from the acid catalyzed reaction of thiocyanate salts (15). No further studies have confirmed this suggested mechanism. However, the emission of high mixing ratios of OCS from teflon filters could be related to a similar production mechanism, as OCS production continued for a number of days and was increased in warmer, and slightly more humid, daylight conditions. There is limited literature on the heterogeneous production of OCS and potential mechanisms should be investigated in future studies. Data with contaminated filter production of OCS have been removed from further analysis and from Figure S1.

Materials for the instrumental setup were carefully chosen to ensure no artificial production of OCS in the system. Testing showed that OCS was produced by rubber diaphragms in pumps and resulted in strong OCS production (pulses up to 24 ppb) in re-circulating soil chambers at Harvard Forest. No soil chamber data was used in the analysis presented here. Neoprene and plastic tubing, which are often used in soil chambers, were particularly strong producers of OCS. Clean Synflex® and Teflon tubing were not found to produce observable OCS. While steps have been taken to minimize the impact of material contamination and to remove any data influences by atmospheric contamination, it is possible that the large OCS emission observed in July may be the result of some unknown physical production mechanism.

In a wheat field Maseyk et al [2014] observed OCS emission of 217 μgS m^{-2} over the final 10 days of measurements (from a total of 657 μgS m^{-2} over 7 weeks). We estimate a comparable OCS emission of 207 μgS m^{-2} over the 10 days of observed net OCS emission at Harvard Forest. The metabolism of sulfur containing amino acids, which increases with temperature and plant stress, may lead to OCS production (Maseyk et al 2014) in a similar manner to CO (Conrad and Seiler (1985)) and CH$_4$ production (Nisbet et al (2008)) from thermal degradation.

Soil warming and nitrogen fertilization experiments have been conducted in plots to the SW of the tower from 2006 to present, including during 2011 {Contosta:2011dh, Contosta:2012kr}. These experiments use ammonium nitrate (NH$_4$NO$_3$) to fertilize 12 plots of size 3 x 3 m. The fertilizer contains trace levels of sulfur (approximately 0.002% sulfur as SO$_4^-$), which is equivalent to an application of 2.2 gS ha^{-1} yr^{-1}, a less than 0.01% increase on the sulfur content of the

soil. The periods of OCS emissions were not found to correlate with the application of the fertilizer. While we cannot discount the possibility of an OCS artifact from the fertilizer, we suspect that the small area involved and the low levels of sulfur application are too small to contribute to the observed OCS signal. Nitrogen fertilization experiments also found increased OCS emission from soils {Mellillo:1989ud} but we do not see a correlation with soil temperature and the related increase in microbial activity. It is possible that the sulfur present in the soils at Harvard Forest, like the soils of the wheat fields in Oklahoma {Maseyk:2014jl}, is a source of OCS through some unknown biophysical mechanism.

S2 Site Description and Ancillary Measurements

S2.1 SITE DESCRIPTION

Measurements were made at the Environmental Measurement Site (EMS) at Harvard Forest, Petersham, MA (42.54°N, 72.17°W, elevation 340 m). The CO_2 flux into and out of the forest has been measured at this Long Term Ecological Research (LTER) site since 1990 [11]. The 30 m meteorology tower extends about 5 m over the forest canopy and is located on moderately hilly terrain surrounded by several kilometers of relatively undisturbed forest; approximately 80% of the turbulent fluxes are produced within 0.7-1 km of the tower [16]. The basal area (m^2 ha^{-1}) of various tree species within the footprint of the tower is tracked on plots established in 1993 [17]. In 2011, the southwest sector was dominated by deciduous species red oak (20.0% basal area) and red maple (11.8%) with some black oak (2.6%) and ash (2.1%). The northwest sector was more mixed with red oak (17.3%) and hemlock (13.2%) dominating and some red maple (9%), red pine (7.3%) and white pine (5.4%). A dried up pond, that is now an area of new tree growth, was also located in the northwest sector.

Soils at Harvard Forest are acidic and originate from sandy loam glacial till. The diversity and richness of the soil microbial community is somewhat reduced at low soil pH [18] but the soil at Harvard Forest contains representatives of the phyla typical in most soils (Blanchard, personal communication), many of which can encode for one or more carbonic anhydrase enzymes [19].

S2.2 CO_2 FLUX MEASUREMENTS

The CO_2 flux at the EMS tower was measured by eddy covariance as described extensively in previous work [11, 13, 17, 20]. The CO_2 flux term accounts for storage of CO_2

within the canopy as determined from gradient measurements of the CO_2 concentration (21). The daytime respiration of CO_2 is projected from the observed temperature dependence of respiration at night. To estimate gross primary productivity (GPP) from the measured CO_2 flux, we use the difference between the daytime CO_2 flux and the projected daytime respiration (13).

The Hemlock Tower is another flux tower at Harvard Forest located 500m away from the EMS tower in a mature hemlock stand. The CO_2 uptake by conifer species in 2011 was found to be greatest in April, May and June (2.1 - 2.4 g-C m^{-2} day^{-1}) before being drastically reduced in July (0.5 g-C m^{-2} day^{-1}), recovering in August (1.5 g-C m^{-2} day^{-1}) and reducing in the fall (0.4 – 0.6 g-C m^{-2} day^{-1}; September – October). The conifer uptake flux increased again in November (1.1 g-C m^{-2} day^{-1}) with higher air temperatures before essentially stopping in December (0.008 g-C m^{-2} day^{-1}).

S2.3 SAP FLOW MEASUREMENTS

Ecosystem scale flux observations cannot distinguish the canopy flux from the soil flux, since both sinks are located beneath the flux measurement point. Measurements of sap flow through trees (i.e. water uptake by trees) provide understanding of whole-tree transpiration with high temporal resolution when measured continuously throughout the growing season. Because both transpiration and photosynthesis are controlled by stomatal conductance, measurements of sap flow and eddy flux can be combined to understand patterns of canopy carbon uptake (22). We measured rates of sap flow (23) in the dominant (by mass) deciduous tree species (*Quercus rubra* (northern red oak) and *Acer rubrum* (red maple)) in a nearby site at Harvard Forest during a period that overlapped with OCS flux measurements. These measurements provide an indication of tree activity that has been used to understand the observed OCS (and CO_2) fluxes. Two sensors were installed at breast height on six individual red oak red maple trees (24 sensors total).

Sap flow rates in both species began to increase on May 19th, just after bud break. Senescence began around late October, with water uptake by the red oak continuing until about November 13th. Elevated sap flow was generally observed before midnight throughout the growing season before reducing to minimal levels in the early hours of the morning. Figure S5 shows the summer sap flow rates staying high into the late afternoon after both PAR and the water vapor flux began to decrease. The bulk tree activity, as

observed by sap flow rates, showed that the red oaks continued to be active for up to 5 hours into the night before reaching zero.

S3. Additional Methodology

S3.1 OCS:CO$_2$ ATMOSPHERIC RELATIVE UPTAKE (ARU):

The impact of vegetative uptake on ambient OCS mixing ratios can be explored by looking at a ratio of OCS to CO$_2$. The Atmospheric Relative Uptake (ARU) is the seasonal change in the OCS:CO$_2$ uptake ratio (9):

$$ARU = \frac{[OCS]_{max-min}}{[OCS]_{annual\_mean}} \times \frac{[CO_2]_{annual\_mean}}{[CO_2]_{max-min}} \qquad \textbf{(S4)}$$

where $[X]_{max-min}$ is the difference between spring maximum and autumn minimum ambient mixing ratios of OCS and CO$_2$ normalized by their annual mean. We calculate an ARU of 8.5 for 2011, which is similar to the ARU ($\sim$8 ± 2) calculated from a multi-annual analysis of flask data collected at Harvard Forest for 2000-2005 (9).

REFERENCES

1. Nelson DD, McManus JB, Urbanski S, Herndon S, Zahniser MS (2004) High precision measurements of atmospheric nitrous oxide and methane using thermoelectrically cooled mid-infrared quantum cascade lasers and detectors. *Spectrochimica Acta Part A-Molecular and Biomolecular Spectroscopy* 60:3325–3335.

2. McManus JB et al. (2010) Application of quantum cascade lasers to high-precision atmospheric trace gas measurements. *Opt Eng* 49:111124.

3. McManus JB, Zahniser MS, Nelson DD (2011) Dual quantum cascade laser trace gas instrument with astigmatic Herriott cell at high pass number. *Appl Opt* 50:A74–A85.

4. Stimler K, Nelson DD, Yakir D (2009) High precision measurements of atmospheric concentrations and plant exchange rates of carbonyl sulfide using mid-IR quantum cascade laser. *Global Change Biology*.

5. Commane R et al. (2013) Carbonyl sulfide in the planetary boundary layer: Coastal and continental influences. *J Geophys Res-Atmos* 118:8001–8009.

6. Santoni GW et al. (2012) Mass fluxes and isofluxes of methane (CH$_4$) at a New Hampshire fen measured by a continuous wave quantum cascade laser spectrometer. *Journal of Geophysical Research* 117:D10301.

7. Maseyk K et al. (2014) Sources and sinks of carbonyl sulfide in an agricultural field in

the Southern Great Plains. *Proceedings of the National Academy of Sciences*.

8.   Billesbach DP et al. (2014) Growing season eddy covariance measurements of carbonyl sulfide and CO_2 fluxes: COS and CO_2 relationships in Southern Great Plains winter wheat. *Agricultural and Forest Meteorology* 184:48–55.

9.   Montzka SA et al. (2007) On the global distribution, seasonality, and budget of atmospheric carbonyl sulfide (COS) and some similarities to CO_2. *Journal of Geophysical Research* 112:D09302.

10.   Meyers T, Hall M, Lindberg S, Kim K (1996) ScienceDirect.com - Atmospheric Environment - Use of the modified bowen-ratio technique to measure fluxes of trace gases. *Atmospheric Environment*.

11.   Urbanski S et al. (2007) Factors controlling CO_2 exchange on timescales from hourly to decadal at Harvard Forest. *Journal of Geophysical Research* 112.

12.   Meredith LK et al. (2014) Ecosystem fluxes of hydrogen: a comparison of flux-gradient methods. *Atmos Meas Tech* 7:2787–2805.

13.   Goulden ML, Munger JW, Fan S-M, Daube BC, Wofsy SC (1996) Measurements of carbon sequestration by long-term eddy covariance: methods and a critical evaluation of accuracy. *Global Change Biology* 2:169–182.

14.   Wilczak J, Oncley S, Stage S (2001) Boundary-Layer Meteorology, Volume 99, Number 1 - SpringerLink. *Boundary-Layer Meteorology*.

15.   Belviso S, Nguyen BC, Allard P (1986) Estimate of carbonyl sulfide (OCS) volcanic source strength deduced from OCS/CO2 ratios in volcanic gases. *Geophys Res Lett* 13:133.

16.   Sakai R, Fitzjarrald D, Moore K (2001) Importance of Low-Frequency Contributions to Eddy Fluxes Observed over Rough Surfaces. *Journal of Applied Meteorology*.

17.   Barford CC (2001) Factors Controlling Long- and Short-Term Sequestration of Atmospheric CO2 in a Mid-latitude Forest. *Science* 294:1688–1691.

18.   Fierer N, Jackson RB (2006) The diversity and biogeography of soil bacterial communities. *Proceedings of the National Academy of Sciences of the United States of America* 103:626–631.

19.   Smith KS, Jakubzick C, Whittam TS, Ferry JG (1999) Carbonic anhydrase is an ancient enzyme widespread in prokaryotes. *Proceedings of the National Academy of Sciences* 96:15184–15189.

20.   Wofsy SC et al. (1993) Net Exchange of CO_2 in a Mid-Latitude Forest. *Science* 260:1–5.

21.   Hutyra LR et al. (2008) Resolving systematic errors in estimates of net ecosystem exchange of CO2 and ecosystem respiration in a tropical forest biome. *Agricultural and Forest Meteorology* 148:1266–1279.

22.   Tang J et al. (2006) Sap flux–upscaled canopy transpiration, stomatal conductance, and water use efficiency in an old growth forest in the Great Lakes region of the United States. *Journal of Geophysical Research* 111:G02009.

23.   Granier A (1987) Evaluation of transpiration in a Douglas-fir stand by means of sap flow measurements. *Tree Physiology* 3:309–320.

Figure Legends

Figure S1: Comparison of OCS (pptv; pmol mol^{-1}) measured by the TILDAS (30 minute average (black) with 1σ standard deviations shown in grey), NOAA flask pair means (red points, 1σ standard deviations shown as red lines error bars (barely visible)) and co-sampled TILDAS OCS (3 hour average at the time of the flask sample (grey circle)). The flasks were sampled weekly followed by analysis by gas chromatography mass spectrometry (GC-MS) in Boulder - as part of the NOAA flask sample network (9).
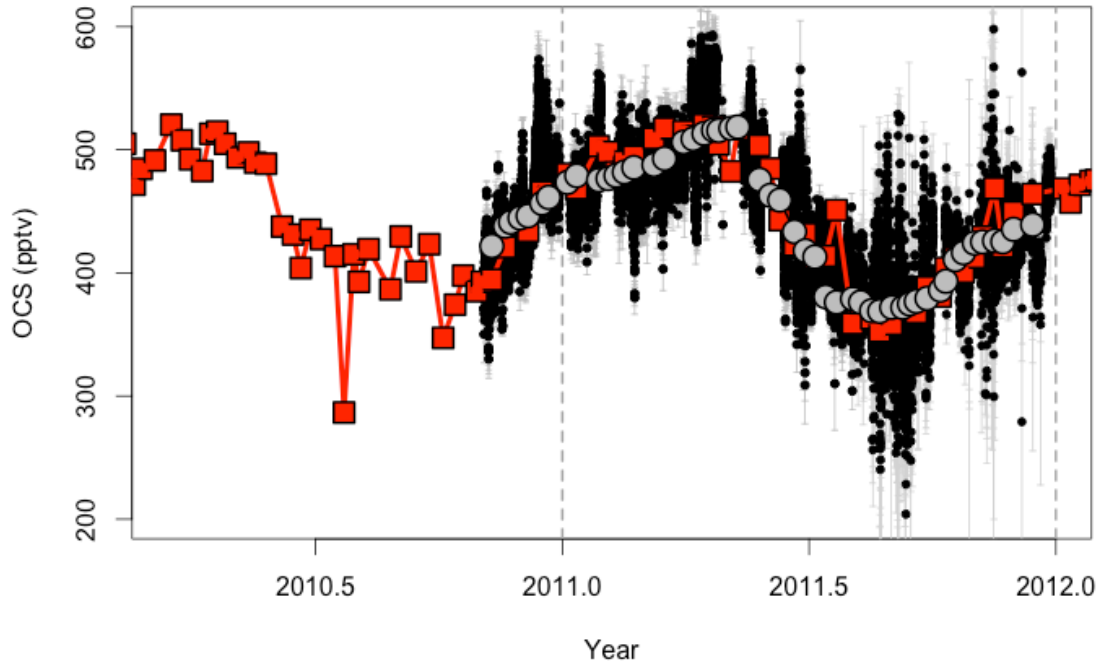
Figure S2: Components of gradient-flux calculated OCS flux for June 14, 2011: (a) gOCS: OCS gradient (black, pptv m^{-1}), confident intervals of the OCS gradient (grey bars, which are barely visible) (b) gH_2O: H_2O gradient (dark blue, pptv m^{-1}), confident intervals of H_2O gradient (grey bars)(c) FH_2O: H_2O flux (blue, mmol m^{-2} s^{-1}), 15% error on eddy covariance measurements (grey bars), (d) gFOCS: OCS gradient – flux (pmol m^{-2} s^{-1}), 2 hour average (black), 30 minute gFOCS (grey points with standard error as grey bars), (e) FCO_2: CO_2 flux (as NEE including storage contribution) (μmol m^{-2} s^{-1}), 30 minute FCO_2 (small light green points), 15% error on eddy covariance measurements (green bars), 2 hours mean (dark green points).
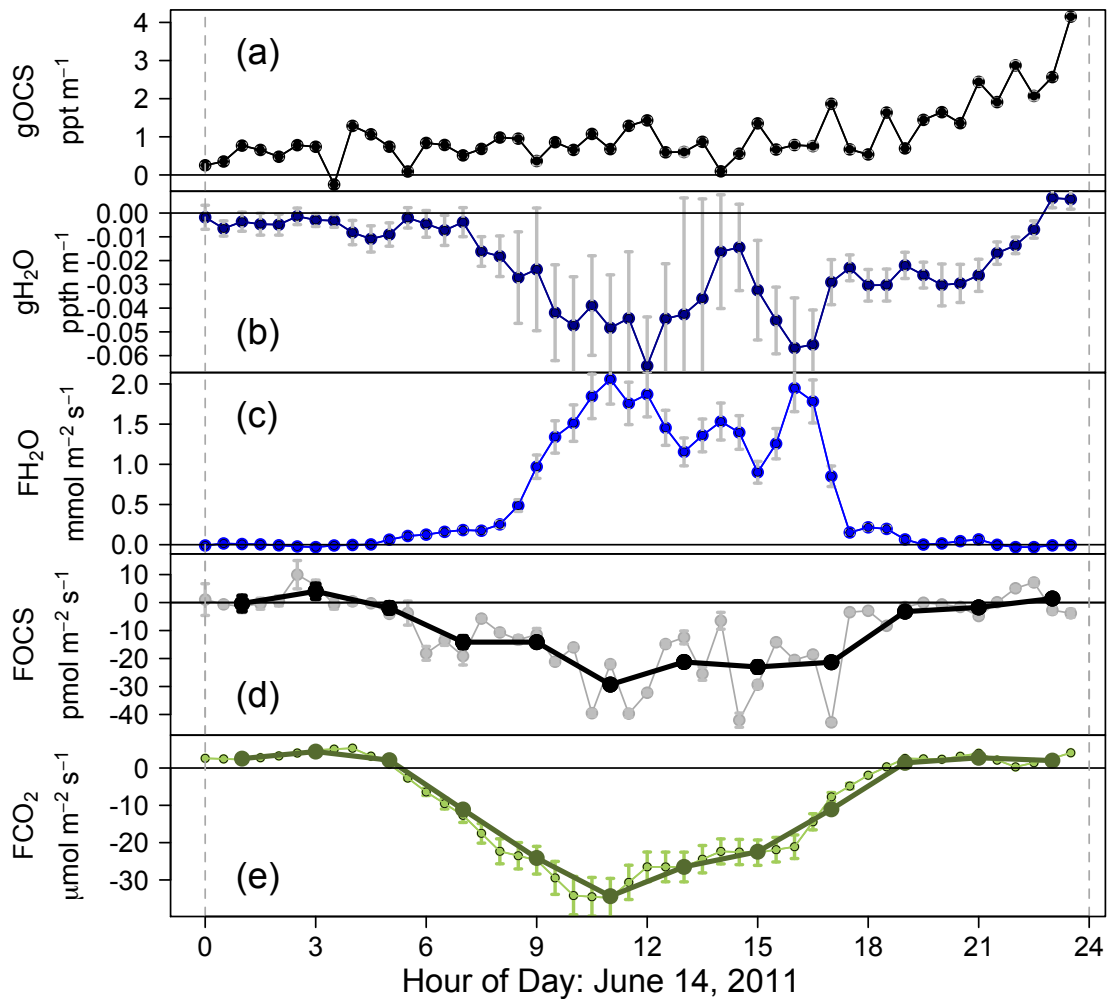
Figure S3: Composite diel cycle of the gradient-flux OCS (gF$_{OCS}$, black points) and eddy covariance OCS flux (eF$_{OCS}$, red squares) for coincident data in 2 hourly time bins for 6 – 12 August 2011. The error bars indicate the 95% confidence intervals of the data within the composite two-hour period.
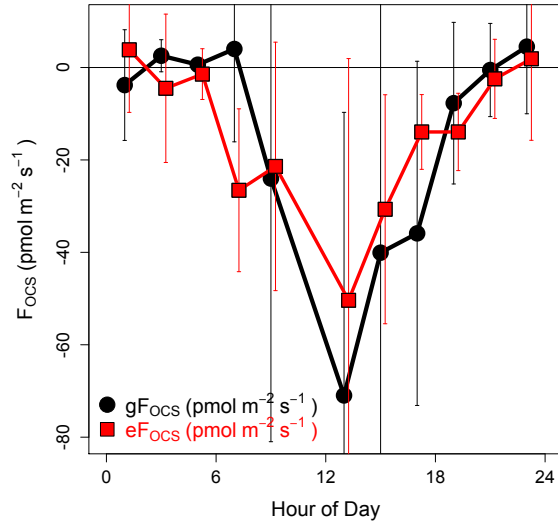
Figure S4: Diurnal composite of OCS (black) and CO₂ (green) fluxes (Eastern Standard Time) for the summer months of 2011: (a1) June, (b1) August, (c1) September, with times of low turbulence ($u* < 0.17$ m s⁻¹) removed. 95% confidence intervals for each species are shown as black error bars. The 95% confidence intervals for CO₂ are barely visible. Both columns show PAR (solid orange line; 10^{-8}E m⁻² s⁻¹) on two different scales. The right column (a2, b2, c2) shows the sap flow rates for oak (brown triangles; gH₂O m⁻² s⁻¹), the vapor pressure deficit (magenta dashed line; Pa), the water vapor flux (blue/navy circles; 5 mmol m⁻² s⁻¹ (multiplied by 5 for graphing)).
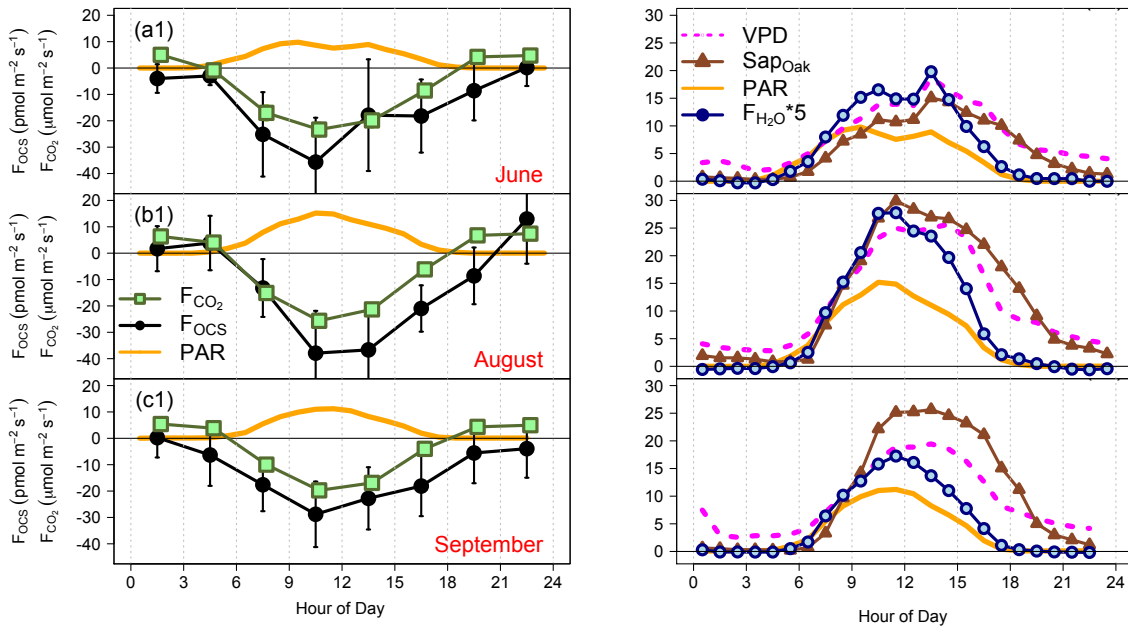
Figure S5: The OCS (black circles; pmol m^{-2} s^{-1}) flux, CO_2 flux (green square; μmol m^{-2} s^{-1}) and the air temperature (blue diamonds, °C) for given surface soil temperatures in December 2011. The data is partitioned to have equal numbers of data points for each temperature shown.
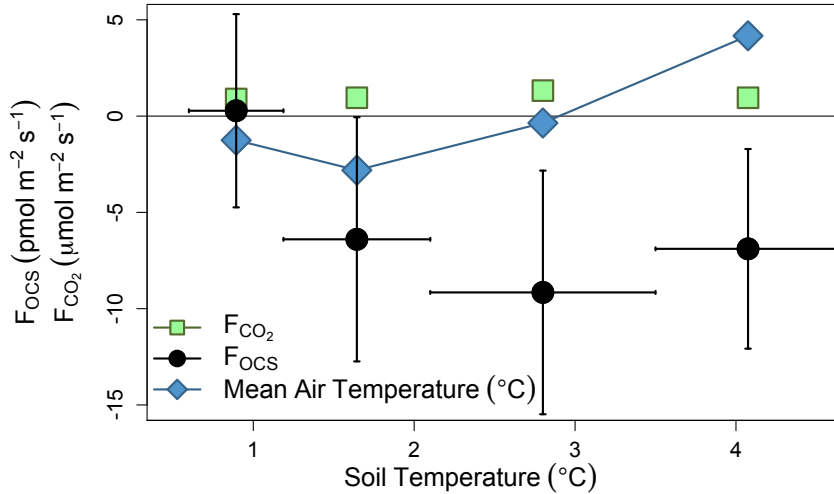
Figure S6: Monthly mean observed OCS fluxes (black; pmol m^{-2} s^{-1}) and SiB simulated OCS fluxes (red; pmol m^{-2} s^{-1}) were compared for (a) night and (b) daytime (Par > 600 μE m^{-2} s^{-1}). This version of SiB includes explicit representation of OCS uptake by soils and vegetation, but does not yet simulate the processes responsible for production of OCS in the ecosystem. Work is underway to consider the night-time OCS uptake and OCS emission processes.